

In vivo visualisation of nanoparticle entry into central nervous system tissue

Petra Henrich-Noack · Sylvia Prilloff · Nadine Voigt ·
Jing Jin · Werner Hintz · Jürgen Tomas ·
Bernhard A. Sabel

Received: 20 October 2011 / Accepted: 1 March 2012 / Published online: 16 March 2012
© Springer-Verlag 2012

Abstract Because the potential neurotoxicity of nanoparticles is a significant issue, characterisation of nanoparticle entry into the brain is essential. Here, we describe an in vivo confocal neuroimaging method (ICON) of visualising the entry of fluorescent particles into the parenchyma of the central nervous system (CNS) in live animals using the retina as a model. Rats received intravenous injections of fluorescence-labelled polybutyl cyanoacrylate nanoparticles that had been synthesised by a standard miniemulsion polymerisation process. We performed live recording with ICON from before and up to 9 days after particle injection and took photomicrographs of the retina. In addition, selective retrograde labelling of the retinal ganglion cells was achieved by stereotaxic injection of a fluorescent dye into the superior colliculus. Using ICON, we observed vascular kinetics of nanoparticles (wash-in within seconds), their passage to the retina parenchyma (within minutes) and their distribution (mainly cellular) under in vivo conditions. For the detection of cell loss—which is important for the evalu-

ation of toxic effects—in another experiment, we semi-quantitatively analysed the selectively labelled retinal neurons. Our results suggest that the dye per se does not lead to neuronal death. With ICON, it is possible to study nanoparticle kinetics in the retina as a model of the blood-brain barrier. Imaging data can be acquired within seconds after the injection, and the long-term fate of cellular uptake can be followed for many days to study the cellular/extracellular distribution of the nanoparticles. ICON is thus an effective and meaningful tool to investigate nanoparticle/CNS interactions.

Keywords Polybutyl cyanoacrylate nanoparticles · Blood-brain barrier · Blood-retina barrier · In vivo confocal neuroimaging · Brain

Introduction

There is an ongoing debate whether nanoparticles are toxic to cells or body organs, but so far toxicological effects were mainly studied in the gastrointestinal system and in the lung. Here, pathophysiological changes after different environmental exposures (inhalation, food) were analysed. However, there are very few studies on the effects of nanoparticles on tissue of the central nervous system (CNS).

Oberdörster et al. (2004), for example, studied nanoparticle absorption by nasal mucosa and subsequent transport via the olfactory bulb to the CNS, but a potential toxicity of nanoparticles on the brain has not been described. In addition, while on the one hand, investigating the non-intentional, undesirable exposure of neurons and glial cells to nanoparticles is important; on the other hand, there is also a “desirable” nanoparticle transfer which needs to be understood (Kreuter 2004). Here, nanoparticles may be an

This article is published as a part of the Special Issue “Nanotoxicology II” on the ECETOC Satellite workshop, Dresden 2010 (Innovation through Nanotechnology and Nanomaterials + Current Aspects of Safety Assessment and Regulation).

Electronic supplementary material The online version of this article (doi:10.1007/s00204-012-0832-4) contains supplementary material, which is available to authorized users.

P. Henrich-Noack (✉) · S. Prilloff · N. Voigt · B. A. Sabel
Institute of Medical Psychology, Otto-von-Guericke University,
Leipziger Str. 44, 39120 Magdeburg, Germany
e-mail: petra.henrich-noack@med.ovgu.de

J. Jin · W. Hintz · J. Tomas
Institute of Mechanical Process Engineering, Otto-von-Guericke
University, Leipziger Str. 44, 39120 Magdeburg, Germany

attractive tool for the pharmaceutical industry to transport drugs across the blood-brain barrier (BBB) into the CNS parenchyma and, obviously, the efficacy and safety and tolerability of these carriers also have to be taken into account.

Brain tissue is very vulnerable to toxic influences, and therefore brain cells such as neurons or glia are well protected by BBB, which keeps potentially harmful molecules out of the brain parenchyma. However, because nanoparticles may be able to cross the BBB by a yet unknown mechanism, we need to learn more about their transport across this biological barrier and to study their influences on the brain. Therefore, appropriate animal models are needed to study the safety and tolerability of nanoparticles in CNS tissue and their passage across the BBB.

In the CNS, walls of cerebral arteries are—unlike peripheral vessels—very tight and their endothelial cells possess various efflux pumps to ensure that only certain substances (including nutrients) can enter the brain (Pardridge 1998, 2002; Saunders et al. 1999; Engelhardt 2003). To analyse the ability of molecules to cross the BBB, the *in vivo* method of “brain/plasma ratio” is the most widely used (Reichel 2006). Other methods are “*In situ* brain perfusion”, “brain uptake index” or microdialysis, but they are less widely used because of their experimental complexity (Dagenais et al. 2000; Elmquist and Sawchuk 1997). There are also various *in vitro* test systems, but they are not yet sufficiently developed to provide reliable answers (Reichel et al. 2003). The existing *in vivo* techniques of measuring the penetration of a drug or carrier into the brain have the disadvantage that they require large numbers of animals and show considerable inter-animal variability. The reason is that for each single data analysis point and each dose, animals have to be killed. These methods are therefore not only inefficient but also result in a relatively large variability of group data, and as a consequence, the power of the existing animal models is too low to study kinetics of transport across the BBB. Moreover, there is no option to study cellular distribution of compounds in the living CNS and, most importantly, there is little information concerning potential cellular damage induced by nanoparticles in such models.

To overcome these limitations of existing models, we have now developed a new technique to visualise and analyse repetitively the passage of fluorescent carriers across the blood-retina barrier (BRB) in living animals.

The BRB is a useful model for the BBB because retinal tissue is ontogenetically derived from the CNS and the function of the BRB is virtually identical with that of the BBB (Steuer et al. 2004, 2005). To visualise nanoparticles and their transport across the BRB, we used the transocular *in vivo* confocal neuroimaging (ICON) technique (Sabel et al. 1997; Prilloff et al. 2010). ICON allows observations of the retina with cellular resolution as well as the study of

the distribution of fluorescent nanoparticles in living CNS tissue. In addition, ICON is a very sensitive method to study cell survival.

We investigated polybutyl cyanoacrylate nanoparticles (PBCA NPs) because they can be reliably loaded with fluorescent dyes and they are able to cross the BBB (Kreuter et al. 2002; Reimold et al. 2008, Schröder and Sabel 1996; Darius et al. 2000; Schröder et al. 2000; Schneider et al. 2008). Though no CNS toxicity has been reported for PBCA NP (Kreuter et al. 2003), they are nevertheless an excellent model to study the BBB passage.

As we now show, ICON is useful to visualise the *in vivo* transport of fluorescent-labelled nanoparticles across the BBB in real time and to visualise neuronal degeneration.

Materials and methods

Rhodamine-labelled PBCA NP

Materials

n-Butyl-2-cyanoacrylate monomer (BCA) was obtained from Henkel Loctite. Lutrol F68 (Poloxamer 188) was purchased from BASF, sodium dodecylsulfate SDS (>99 %) and soybean oil (Ph. Eur.) were from Roth, and Rhodamine 123 (>98 %) was received from Biotium. Phosphoric acid and ammonia solution were of pure grade. All chemicals were used as received. Distilled water was used for all preparations.

Experimental procedure

Rhodamine-labelled PBCA NPs were synthesised by a standard miniemulsion polymerisation process. O/W miniemulsion was made from two solutions:

Solution (I)—aqueous phase: 0.018 g Rhodamine 123, 0.06 g Lutrol F68, and 0.024 g sodium dodecylsulfate were dissolved in 4.8 ml phosphoric acid (0.1 mol l^{-1}).

Solution (II)—oil phase: 0.072 g soybean oil was mixed with 1.2 g n-Butyl-2-cyanoacrylate monomer and cooled down to 4°C .

Solution (I) was added just prior ultra sonication to solution (II). The two-phase mixture was sonicated with a Bandelin Sonopuls HD 70 sonifier (70 % amplitude) for 4 min under ice cooling. Thirty seconds after sonication, the polymerisation process was induced by pouring the miniemulsion into 4.8 ml ammonia solution (0.1 mol l^{-1}) while stirring on a magnetic stirrer. After 5 min, the pH was adjusted to 7.0. PBCA NP suspension was kept at 6°C under protection from light. The solid content of the suspension was 80 mg ml^{-1} .

Characterisation of nanoparticles in suspension

The particle size distributions of the PBCA NPs in suspension were measured using the photon correlation spectroscopy (Model Zetasizer Nano ZS, Malvern Instruments, UK, He–Ne laser $\lambda = 633$ nm, scattering angle 173° , at 25°C). Stability of the particles against agglomeration was evaluated using the zeta potential (Zetasizer Nano ZS, Malvern Instruments, UK).

Particle size distributions

In Fig. 1, the number- as well as the volume-based particle size distributions, $Q_0(d)$ and $Q_3(d)$ of Rhodamine 123-labelled PBCA NPs and of non-modified PBCA NPs (without Rhodamine 123) are shown. Rhodamine 123-labelled PBCA NPs have a mean particle size of 68.9 nm (number mean), and 149.8 nm (volume mean), respectively. Polydispersity index PDI is 0.190, obtained from photon correlation spectroscopy. Fluorescence marker Rhodamine 123 has almost no influence on the particle sizes, as shown in Fig. 1. Non-modified PBCA NPs have a mean diameter of 51.3 nm (number mean), as well as of 167.6 nm (volume mean). Polydispersity index PDI is 0.210.

Zeta potential

For the nanocolloidal PBCA NPs, the zeta potential was determined, ranging from -42.5 to -47.5 mV. Thus, a long-term stability of manufactured NPs is possible.

Surgery

Male Lister hooded rats (CrI: LIS; Charles River; ordered at 6–7 weeks of age) were kept at $24\text{--}26^\circ\text{C}$ environmental

temperature, 50–60 % humidity, 12-h dark/light cycle and free access to food and water. On the day before surgery, food was removed to facilitate general narcosis (description see below). All animal experiments were carried out according to the Protection of Animals Act (as amended on 25 May 1998) and according to the requirements of the German National Act on the use of experimental animals.

To analyse the kinetics of the nanoparticle distribution and absorption, the animals were anaesthetised with an i.p. injection of Ketanest (50 mg/kg; Parker-Davis, Berlin, Germany) and Rompun (15 mg/kg; Bayer Vital GmbH, Leverkusen, Germany). Thereafter, they were placed on a custom-built table and positioned under a confocal microscope (LSM 5 Pascal; Carl Zeiss MicroImaging GmbH, Jena, Germany), and the head of the rat was fixed with a head-holder. Nanoparticles were then injected intravenously with a single dose of 0.1 ml/100 g body mass into the tail vein via a pre-implanted catheter just prior to the imaging session.

In order to quantify neuronal cell death in the retina, we selectively labelled retinal ganglion cells by retrograde transport via the optic nerve. To this end, we injected a fluorescent dye (Mini Emerald; Invitrogen, Karlsruhe, Germany) into the superior colliculus. The animals were fixed in a stereotaxic frame after being anaesthetised as described above (Ketanest/Rompun). After drilling two holes into the skull (coordinates: 1.2 mm from Sutura sagittalis; 6.9 mm posterior to Bregma), 2 μl solution (5 % Mini Emerald) was injected into the brain with a Hamilton syringe (0.5 μl at 4, 3.5, 3, 2.5 mm from skull; microlitre 700 series syringe; Hamilton, Reno NV, US). After 7 days, a baseline ICON recording was performed and the number of labelled neurons was quantified in the region of interest (details see below). One week after ICON, traumatic injury was induced by optic nerve crush. Briefly, under a binocular microscope, the optic nerve was approached from the orbita by a lateral canthotomy and an incision of the conjunctiva lateral to the cornea. The retractor bulbi muscle was separated and the optic nerve exposed. The nerve was then crushed with a calibrated forceps for 30 s (Sautter and Sabel 1993). After completion of the crush, an antibiotic eye ointment (Aureomycin) was topically applied to prevent inflammation.

After 3 and 15 days, the number of retinal ganglion cells was counted again after ICON.

ICON

ICON uses the animals' own eye as part of the optical apparatus to visualise living cells in the retina. The rats were anaesthetised as described above (Ketanest/Rompun) and then positioned underneath a standard confocal laser scanning microscope (LSM 5 Pascal; Carl Zeiss MicroImaging

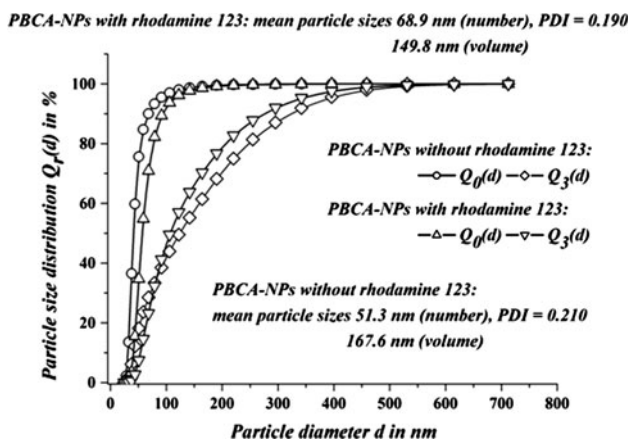


Fig. 1 The particle size of the PBCA NP with and without Rhodamine 123 loading was determined by photon correlation spectroscopy. The plot demonstrates that Rhodamine 123 has no significant influence on the particle size distribution

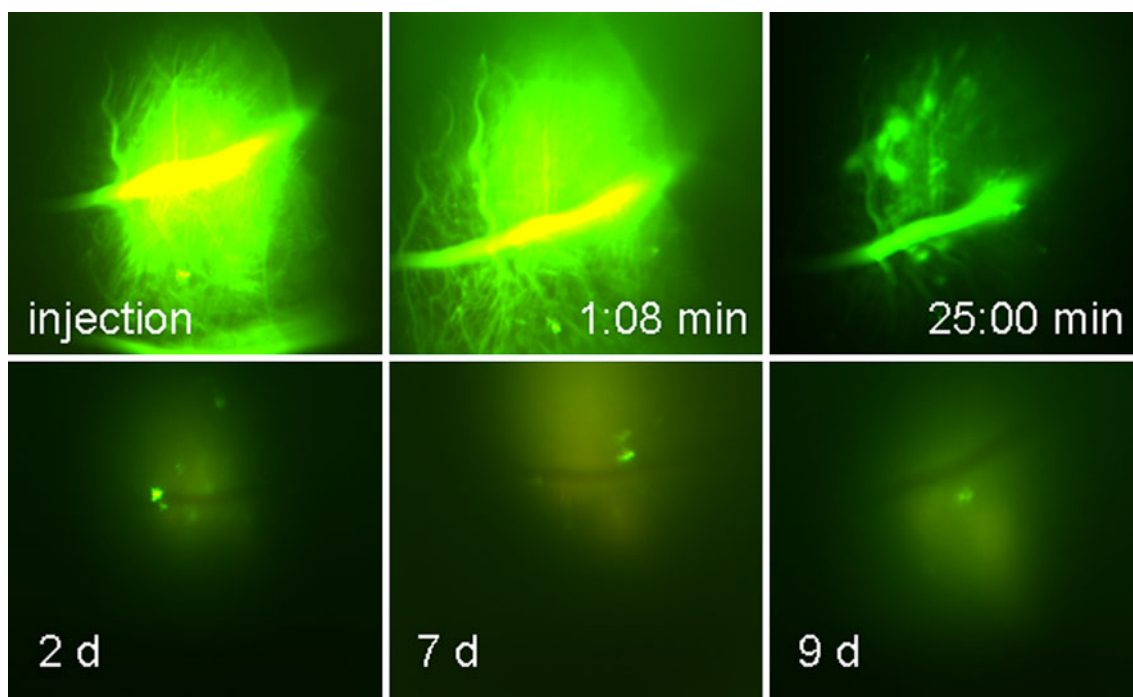


Fig. 2 These photomicrographs illustrate the intensive vascular fluorescence signal during the wash-in phase after i.v. injection of the nanoparticle formulation. At 25 min post-injection, clear cellular labelling is detectable (round dots above the still fluorescent vessel). Also,

on days 2, 7 and 9, cellular labelling in the parenchyma can be seen; however, we can only speculate on whether PBCA NP themselves are present or only the fluorescent dye

GmbH, Jena), which is equipped with a large probe space so that the long working distance objective lens could be positioned directly above the contact lens on the rat's eye. The eyes were treated with Neosynephrine-POS 5 % (Ursapharm, Saarbrücken) to relax the iris. Vidisic optical gel (M. Pharma, Berlin) was applied as an immersion medium for the contact lens (Hruby style –80 dioptrin planoconcave lens; Newport GmbH, Darmstadt), which adjusted the path of the laser ray onto the retina.

To follow changes over time, we determined under the microscope a well-defined region of interest that contained a sufficient number of cells that could easily be identified again using blood vessel morphology as landmark criteria. To study the blood-retina barrier transfer, fluorescent nanoparticles were injected into the tail vein and the fluorescent signal was then monitored. We used PBCA-Rhodamine formulations with negative zeta potential (Capsulation Pharma AG, Berlin) and injected 0.1 ml/100 g bodyweight of a solution with a nanoparticle concentration of 25–80 mg/ml (number of animals $n = 7$). As a control, animals received a solution with Rhodamine 123 only (number of animals $n = 4$). The animals were imaged immediately after injection and on day 2 and day 7. Recording with a CCD camera (AxioCam MRc, Carl Zeiss MicroImaging GmbH, Jena) started immediately after injection, and confocal images were taken at 25 min post-injection and on days 2, 7 and 9.

Results

Nanoparticle kinetic

Fluorescence of Rhodamine-labelled PBCA NP (negative zeta potential, with coating) was visible in the blood vessels a few seconds after the injection in the tail vein (see Fig. 2 and supplementary material (film)). The peak fluorescence intensity was within 6 s after i.v. injection, but the fluorescent intensity decreased in the large vessels while leaving a weaker staining in the small vessels. Clear cellular labelling was not yet detected at this early time point. During the next 20–25 min, we collected confocal images of the retina and detected fluorescence signals in the parenchyma, indicating that PBCA NP had crossed the BRB. These signals accumulated in the cells rather than in the extracellular space. The number of labelled cells increased within the 20- to 25-min recording time.

Imaging the same region of interest repetitively with ICON, we could demonstrate that many cells were still clearly labelled 48 h after injection, whereas the nanoparticles were cleared completely from the blood as no fluorescence was detectable in the lumen of the vessels. Even after 9 days, we still could detect a few labelled cells in the retina.

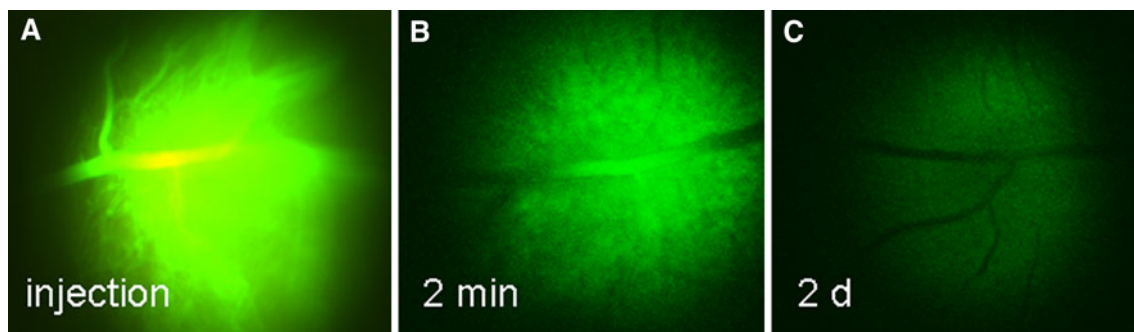
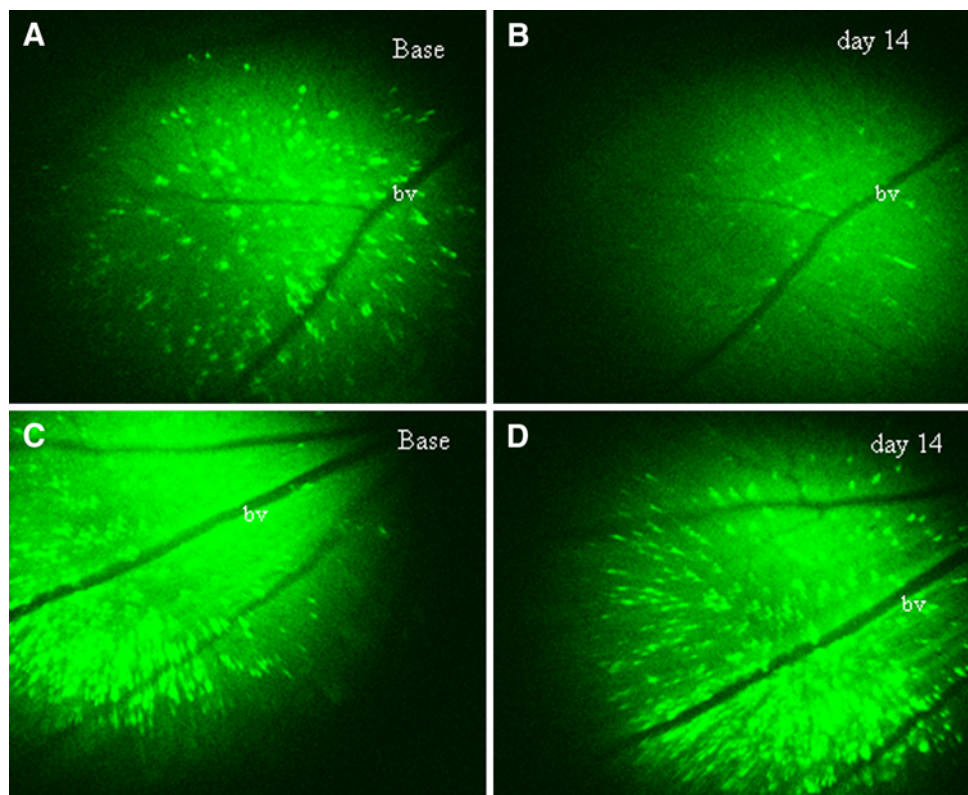


Fig. 3 This figure is a typical example of a control experiment where animals received i.v. injections of a Rhodamine 123 solution only without any PBCA NP. Clearly, no cellular labelling appears

Fig. 4 These photomicrographs show retinal ganglion cells labelled retrogradely with a fluorescent dye after injection of the tracer into the superior colliculus. **a** and **c** are baseline recording. In **b** significantly fewer cells can be seen in comparison with **a**, indicating that the trauma-induced cell death is clearly detectable. For comparison, control animals do not reveal any changes in the number of labelled cells, which indicates that the labelling with this fluorescent dye per se is not toxic. *bv* blood vessel



Injections of Rhodamine alone did not lead to any fluorescence signal outside the vessels (see Fig. 3).

Detection of neuronal death

Imaging of the retinal ganglion cells with ICON revealed that many had degenerated retrogradely after the optic nerve crush. In comparison with the baseline recording, the number of cells was reduced significantly on day 3 and day 15 after the trauma by 15.5 and 60.6 %, respectively (see Fig. 4a, b). In control animals without traumatic lesion, the number of retinal ganglion cells quantified in the region of interest did not change (see Fig. 4c, d).

Discussion

We used ICON to study the passage of nanoparticles across the blood-retina barrier (BRB), because the structure and function of the BRB and the BBB are essentially the same. The retina is ontogenetically derived from brain tissue and—from a theoretical point of view—just as brain tissue, it needs to maintain a tight homeostasis of the extracellular and intracellular milieu. This view is supported by experiments from Steuer et al. (2004) who suggests that the function of the BRB and BBB is very similar, if not identical: they compared the function of the BBB and BRB by studying the passage of different pharmacological active

compounds and found both to be similar, which suggests that the BRB can be used as a model for the BBB. Moreover, Steuer et al. (2005) showed that the BRB and BBB are also structurally similar: in both organs, tight junctions are present and both have the typical efflux systems (permeability-glycoprotein and multidrug-resistant protein).

Based on these considerations, we propose to use ICON imaging of the retina as a model of the BBB and also as a model for live imaging of neurotoxicity. The major advantages of using ICON for the analysis of nanoparticle kinetic and toxicity in the CNS are as follows:

1. the kinetic of BBB passage can be followed repetitively in living animals,
2. fast and high-frequency data collection immediately (seconds) after injection and for an extended period of time is possible,
3. parallel acquisition of data regarding kinetic and neuronal damage,
4. and morphological features of fluorescent cells can be observed and quantified such as cell size (Rousseau et al. 1999; Rousseau and Sabel 2001), calcium activation (Prilloff et al. 2007) and extracellular/intracellular distribution of labelled nanoparticles or compounds.

These are unique advantages of retinal imaging with ICON in comparison with other methods, which were predominantly developed for purposes such as analysing the transport of compounds/carriers into the brain (e.g. brain/plasma ratio; see chapter “Introduction”). In addition, these other methods have the limitations that they require a greater number of animals, they are more restricted regarding data collection points (e.g. they not provide values immediately after injection), they do not provide information about the morphological distribution and they do not provide evidence regarding neuronal degeneration.

ICON was established several years ago in our laboratory to investigate neurophysiological and pathophysiological issues and this method was found to be feasible for real-time observations of neuronal damage, and morphological changes such as cell size and activation changes of calcium-labelled cells (Prilloff et al. 2010, 2007; Sabel et al. 1997; Rousseau et al. 1999; Rousseau and Sabel 2001). Also, we accomplished double-labelling of healthy and degenerating retinal ganglion cells with two different fluorescent markers (Prilloff et al. 2010). Therefore, this imaging technique is able to capture toxicity-induced neurodegeneration (e.g. using green fluorescence) in parallel to the analysis of the fluorescent nanoparticle kinetic (e.g. with red fluorescence like Rhodamine). With the fluorescent dyes chosen so far (Rhodamine, Fluoresceine), no toxic effects have been detected (Prilloff et al. 2010) and our results presented here do also not show any cell loss due to the labelling method itself either.

According to the experience from our group and others, the nanoparticles used in the current work (PBCA NP) were unlikely to induce cell death (Kreuter et al. 2003). This is in agreement with the fact that PBCA NP have been used already in clinical trials (Zhou et al. 2009). We therefore damaged retinal neurons by traumatic injury and detected—as expected—massive cell loss afterwards (Fig. 4). However, the control group did not show significant changes in the signal; therefore, we suggest that the labelling and imaging method itself does not influence the results of toxicity studies.

The unique feature of our technique of *in vivo* nanoparticle imaging with ICON is the synopsis of kinetic and anatomical imaging. In the current ICON experiments, we were able to define the spatial distribution (cellular/extracellular) of the PBCA NP fluorescence. Although the photomicrographs clearly show an intracellular localisation, we can not yet identify the kind of cells which had been labelled (e.g. glia? neurons?). However, when combined with retrograde labelling of retinal ganglion cells, it will be possible to detect *in vivo* whether the nanoparticles have been taken up by these neurons. Moreover, for defining the cell type containing nanoparticles, the standard immunohistochemistry method of *ex vivo* double-labelling of retinal explants can be applied at the end of the *in vivo* analysis.

Currently, narcosis is the limiting factor regarding the period and the frequency of data collection. The *i.p.* injection of the Ketanest/Rompun cocktail usually provides a time frame of 40 min deep narcosis for recording. Unfortunately, rats do not tolerate well a follow-on anaesthesia within the next 1–2 days. Using other ways of anaesthetising as for example with inhalation narcosis (Isofluran), may allow extending the imaging period to several hours and may also allow a higher frequency of measurements. However, although the ICON procedure is not invasive or painful, superficial anaesthesia is clearly not enough as any eye movements of the animals need to be completely avoided to be able to take proper microphotographs of the retina.

Another critical issue to be discussed is the possible dissociation of the fluorescent dye and the nanoparticles. For interpreting the results correctly, the stability of the nanoparticle/dye formulation has to be tested beforehand. The PBCA NP have been shown not to disintegrate for months when stored in the refrigerator (Sommerfeld et al. 2000). However, in biological systems, PBCA NP are known to undergo enzymatic ester hydrolysis to yield non-toxic degradation products (butanol and water-soluble poly (2-cyanoacrylic acid); (O’Sullivan and Birkinshaw 2002)). While this is an advantage for drug release, it leaves our kinetic analysis with the uncertainty whether there are particles present at the late data collection points (9 days) or whether the fluorescent signal is the result of just free floating fluorescent dye. However,

the latter is rather unlikely because free dye would be absorbed rather fast.

In summary, we demonstrated that absorption and distribution of PBCA NP in the brain can be analysed with ICON, giving us the advantage of (i) *in vivo* imaging of nanoparticle kinetics immediately after application, (ii) repetitive data collection over an extended period of time, (iii) synopsis of kinetic and morphological distribution and (iv) a new model of neurotoxicity. This method is applicable for (i) nanoparticles of any kind which can be loaded with fluorescent dyes, (ii) nanoparticles which are fluorescent themselves, (iii) quantum dots and (iv) basically any compound which emits an appropriate and sufficient fluorescent signal.

Conflict of interest We have no conflict of interest.

References

- Dagenais C, Rousselle C, Pollack GM, Scherrmann JM (2000) Development of an *in situ* mouse brain perfusion model and its application to mdr1a P-glycoprotein-deficient mice. *J Cereb Blood Flow Metab* 20:381–386
- Darius J, Meyer FP, Sabel BA, Schroder U (2000) Influence of nanoparticles on the brain-to-serum distribution and the metabolism of valproic acid in mice. *J Pharm Pharmacol* 52:1043–1047
- Elmqvist WF, Sawchuk RJ (1997) Application of microdialysis in pharmacokinetic studies. *Pharm Res* 14:267–288
- Engelhardt B (2003) Development of the blood-brain barrier. *Cell Tissue Res* 314(1):119–129
- Kreuter J (2004) Nanoparticles as drug delivery system. In: Nalwa HS (ed) *Encyclopedia of nanoscience and nanotechnology*, vol 7. American Scientific Publishers, New York, pp 161–180
- Kreuter J, Shamenkov D, Petrov V, Rame P, Cychutek K, Koch-Brandt C, Alyautdin R (2002) Apolipoprotein-mediated transport of nanoparticle-bound drugs across the blood-brain barrier. *J Drug Target* 10:317–325
- Kreuter J, Rame P, Petrov V, Hamm S, Gelperina SE, Engelhardt B, Alyautdin R, von Briesen H, Begley DJ (2003) Direct evidence that polysorbate-80-coated poly(butylacrylate) nanoparticles deliver drugs to the CNS via specific mechanisms requiring prior binding of drug to the nanoparticles. *Pharm Res* 20:409–416
- O'Sullivan C, Birkinshaw C (2002) Hydrolysis of poly(n-butylcyanoacrylate) nanoparticles using esterase. *Polym Degrad Stab* 78:7–15
- Oberdorster G, Sharp Z, Atudorei V, Elder A, Gelein R, Kreyling W, Cox C (2004) Translocation of inhaled ultrafine particles to the brain. *Inhal Toxicol* 16:437–445
- Pardridge WM (ed) (1998) *Introduction to the blood-brain barrier: methodology, biology and pathology*. University Press, Cambridge
- Pardridge WM (2002) Drug and gene targeting to the brain with molecular Trojan horses. *Nat Rev Drug Discov* 1:131–139
- Prilloff S, Noblejas MI, Chedhomme V, Sabel BA (2007) Two faces of calcium activation after optic nerve trauma: life or death of retinal ganglion cells *in vivo* depends on calcium dynamics. *Eur J Neurosci* 25:3339–3346
- Prilloff S, Fan Y, Henrich-Noack P, Sabel BA (2010) *In vivo* confocal neuroimaging (ICON: non-invasive, functional imaging of the mammalian CNS with cellular resolution. *Eur J Neurosci* 31:521–528
- Reichel A (2006) The role of blood-brain barrier studies in the pharmaceutical industry. *Curr Drug Metab* 7:184–203
- Reichel A, Begley DJ, Abott NJ (2003) The blood-brain barrier: biology and research protocols. In: Nag S (ed) *Methods in molecular medicine*. Humana Press, New York, pp 309–326
- Reimold I, Domke D, Bender J, Seyfried CA, Radunz HE, Fricker G (2008) Delivery of nanoparticles to the brain detected by fluorescence microscopy. *Eur J Pharm Biopharm* 70:627–632
- Rousseau V, Sabel BA (2001) Restoration of vision IV: role of compensatory some cell swelling of surviving retinal ganglion cells in recovery of vision after optic nerve crush. *Restor Neurol Neurosci* 18:177–189
- Rousseau V, Engelmann R, Sabel BA (1999) Restoration of vision III: soma swelling dynamics predicts neuronal death or survival after optic nerve crush *in vivo*. *NeuroReport* 10:3387–3391
- Sabel BA, Engelmann R, Humphrey MM (1997) *In vivo* confocal neuroimaging of CNS neurons (ICON). *Nat Med* 3:244–247
- Saunders NR, Habgood MD, Dziegielewska KM (1999) Barrier mechanisms in the brain. *Clin Exp Pharmacol Physiol* 26:11–19
- Sautter J, Sabel BA (1993) Recovery of brightness discrimination in adult rats despite progressive loss of retrogradely labelled retinal ganglion cells after controlled optic nerve crush. *Eur J Neurosci* 5:680–690
- Schneider T, Becker A, Ringe K, Reinhold A, Firsching R, Sabel BA (2008) Brain tumour therapy by combined vaccination and antisense oligonucleotide delivery with nanoparticles. *J Neuroimmunol* 195:21–27
- Schröder U, Sabel BA (1996) Nanoparticles, a drug carrier system to pass the blood-brain barrier, permit central analgesic effects of *i.v.* dalargin injections. *Brain Res* 710:121–124
- Schröder U, Schröder H, Sabel BA (2000) Body distribution of 3H-labelled dalargin bound to poly(butyl cyanoacrylate) nanoparticles after *i.v.* injection in mice. *Life Sci* 66:495–502
- Sommerfeld P, Sabel BA, Schroeder U (2000) Long-term stability of PBCA nanoparticle suspensions. *J Microencapsul* 17:69–79
- Steuer H, Jaworski A, Stoll D, Schlosshauer B (2004) *In vitro* model of the outer blood-retina barrier. *Brain Res Protoc* 13:26–36
- Steuer H, Jaworski A, Elger B, Kausmann M, Keldenich J, Schneider H, Stoll D, Schlosshauer B (2005) Functional characterization and comparison of the outer blood-retina barrier and the blood-brain barrier. *Invest Ophthalmol Vis Sci* 46:1047–1053
- Zhou Q, Sun X, Zenf L, Liu J, Zhang Z (2009) A randomized multicenter phase II clinical trial of mitoxantrone-loaded nanoparticles in the treatment of 108 patients with unresected hepatocellular carcinoma. *Nanomedicine* 5:419–423